



## Effect of humic acids on the adsorption of paraquat by goethite

Maximiliano Brigante\*, Graciela Zanini, Marcelo Avena

INQUISUR, Departamento de Química, Universidad Nacional del Sur, Av. Alem 1253, 8000 Bahía Blanca, Argentina

### ARTICLE INFO

#### Article history:

Received 30 April 2010

Received in revised form 5 August 2010

Accepted 7 August 2010

Available online 14 August 2010

#### Keywords:

Paraquat

Goethite

Humic acid

Adsorption

Surface complexes

Capillary electrophoresis

### ABSTRACT

The adsorption of the herbicide paraquat ( $PQ^{2+}$ ) on goethite and on the binary system humic acid–goethite has been studied in batch experiments by performing adsorption isotherms under different conditions of pH, supporting electrolyte concentration and temperature. The results were completed with capillary electrophoresis (CE) in order to measure the binding isotherm between  $PQ^{2+}$  and humic acid (HA) molecules in solution.  $PQ^{2+}$  adsorption is negligible on the bare goethite surface but important on the HA–goethite adsorbent. In this last case, the adsorption increases by increasing pH and decreasing electrolyte concentration. There are no significant effects of temperature on the adsorption. The adsorption takes place by direct binding of  $PQ^{2+}$  to adsorbed HA molecules leading to the formation of surface species of the type goethite–HA– $PQ^{2+}$ . The results are consistent with a mechanism where  $PQ^{2+}$  binds negatively charged groups of HA (carboxylates and phenolates) forming ionic pairs or outer-sphere complexes. Since goethite in nature usually contains adsorbed HA molecules, it may act as a good adsorbent for cationic herbicides. This will not only benefit the deactivation of the herbicides but also reduce their leaching and transport through groundwater.

© 2010 Elsevier B.V. All rights reserved.

### 1. Introduction

From its appearance with commercial purposes in 1961, paraquat (1,1'-dimethyl-4,4'-dipyridinium chloride), has become one of the most used herbicides in the world with a variety of applications owing to its physical and chemical properties, such as high solubility in water, low vapor pressure and high binding potential, which make it suitable for many agriculture uses [1]. However, it is known that this herbicide is one of the most toxic poisons if deliberately or accidentally ingested [2]. In recent years, investigations on paraquat toxicity have suggested that this herbicide might be an environmental factor contributing to a neurodegenerative disorder, such as Parkinson's disease [3]. Paraquat ( $PQ^{2+}$ ), also known under the name of methyl viologen, is frequently used as an efficient electron transfer-reagent in electrochemistry and bioelectrochemistry [4]. It is easily reduced to stable, highly colored  $PQ^{+•}$  radical. The herbicidal activity is, in effect, also a consequence of the formation of  $PQ^{+•}$  radicals.

Binding of herbicides to soils and soil components is considered to be the major cause of herbicide deactivation once in soils and it is important both from the point of view of inhibiting herbicides toxic properties and in restricting their transport into water systems [5]. Through adsorption–desorption and precipitation–dissolution reactions, minerals and/or soil organic matter can regulate the con-

centration of  $PQ^{2+}$  and its metabolites in aqueous solutions [6]. However, it is known that the adsorption of  $PQ^{2+}$  varies largely with the nature of the adsorbent.  $PQ^{2+}$  adsorbs strongly on clay minerals and somewhat less on activated carbon and humic substances [7–9]. The adsorption on inorganic oxides seems to be weak, although data about this in the literature are scarce [10].

Goethite ( $\alpha$ -FeOOH) is one of the most common and stable crystalline iron oxide in sediments and natural systems. This mineral has a relative high surface area and high reactivity [11,12] which would be suitable for the adsorption and deactivation of pesticides, nutrients, and hazardous compounds in natural conditions, and may also affect greatly the distribution and transport of contaminants in the environment. Goethite is also found associated with organic matter in soils. This mutual interaction can modify the individual reactivity of both organic matter and the mineral surface affecting the cycle of the various chemical species present in soil [13].

It is known that the adsorption and mobility of different herbicides increase by increasing the organic matter content in soils [14,15]. For soils that have relatively high organic matter levels (>5%), the mobility of the herbicides has been related to the total organic matter content, with the nature of the organic matter having little apparent influence on sorption processes [16]. Humic acids (HAs) represent a very important and active fraction of the organic matter in soils, sediments and water and play a part in many of the physical, chemical and geochemical processes in the natural environment, including the binding and transport of herbicides and pesticides [17,18]. In the case of  $PQ^{2+}$ –HA system, Senesi et

\* Corresponding author. Tel.: +54 291 4595101x3593.

E-mail address: [brigante@uns.edu.ar](mailto:brigante@uns.edu.ar) (M. Brigante).

al. [19] suggested that multiple binding mechanisms may occur in the adsorption process with the formation of (a) ionic bonds between carboxylate groups of HA and the cationic herbicide; and (b) charge-transfer ( $\pi$  bonding) between the aromatic ring of the herbicide and complementary electron-donor or electron-acceptor structural moieties of HA. Brigante et al. [20] also suggested through dissolution experiments that  $PQ^{2+}$  ions can also interact with HA molecules by hydrophobic interactions promoting the dissolution of humic particles.

Various experimental techniques have been used to study HA and their interaction with herbicides, such as NMR [21], mass spectrometry [22], fluorescence spectroscopy [23], infrared spectrophotometry [24], equilibrium dialysis method [25], etc. Capillary electrophoresis (CE) has been found to be one of the most efficient methods for characterization of HA [26,27]. Due to its high sensitivity and efficiency, some physicochemical properties, i.e., aggregation and stability have been studied using this technique [28]. However, despite the high number of studies done and reported in the literature, information concerning the mechanisms of interaction between these pollutants with HA is not well understood and needs to be clarified.

The aim of this article is to present a study of  $PQ^{2+}$  adsorption on goethite and on a HA-modified goethite (HA-goethite). The effects of varying pH, temperature and ionic strength on the adsorption isotherms are investigated. The binding isotherm of  $PQ^{2+}$  to HA molecules in solution is also presented and compared. The obtained results will be useful to gain insights into the general mechanisms involved in the adsorption of  $PQ^{2+}$  to soil and sediment components, and will serve as a basis for further studies evaluating the mobility of herbicides in the environment.

## 2. Materials and methods

### 2.1. Goethite and HA-goethite. Synthesis and general characterization

Goethite was prepared using a procedure similar to that described by Atkinson et al. [29]. Briefly, a 5 M NaOH solution was added dropwise ( $10 \text{ mL min}^{-1}$ ) to a 0.1 M  $\text{Fe}(\text{NO}_3)_3 \cdot 9\text{H}_2\text{O}$  solution until the pH was 12. Carbon dioxide contamination was avoided during the synthesis by bubbling water-saturated  $\text{N}_2$ . The resulting ferrihydrite dispersion was aged at  $60^\circ\text{C}$  in a capped Teflon container during 3 days and then it was washed with doubly distilled water until the conductivity was lower than  $10 \mu\text{S cm}^{-1}$ . After that, the dispersion was freeze-dried in order to obtain a dry powder.

The HA used to modify the goethite was extracted from an alfalfa-cultivated soil (INTA Manfredi experimental station, Córdoba, Argentina) and purified according to the procedures recommended by the IHSS. Its elemental composition is C (54.43%), H (4.00%), N (1.62%), and O (39.95%). The ash content of the sample is 1.18% and the total acidity is  $9.90 \text{ mmol g}^{-1}$  of which  $4.71 \text{ mmol g}^{-1}$  is ascribed to carboxylic groups and  $5.19 \text{ mmol g}^{-1}$  to phenolic groups. More information about the general characteristics of this HA sample can be found elsewhere [30]. The HA-goethite sample was prepared by treating 50 mL of a  $23.17 \text{ g L}^{-1}$  goethite dispersion (pH 8.7 in 0.1 M KCl) with 450 mL of a  $200 \text{ mg L}^{-1}$  HA solution (pH 8.7 in 0.1 M KCl solution). This experiment was carried out in a cylindrical plastic vessel covered with a plastic cap. Mixing was done with a magnetic stirrer, and carbon dioxide contamination was avoided by bubbling water-saturated  $\text{N}_2$ . The mixture was stirred for 4 h at 450 rpm and  $25 \pm 2^\circ\text{C}$  and centrifuged to separate the phases. An aliquot of the supernatant was analyzed to quantify the HA remaining in the supernatant and to calculate the adsorbed amount of HA. The solid was then washed twice with water at

pH 8.7 in order to remove the unadsorbed HA and freeze-dried to obtain a dry powder. The resulting HA-goethite sample contained 48.8 mg of HA per gram of goethite.

Quantification of HA in the supernatant was performed by UV-vis spectroscopy, using an Agilent 8453 UV-Vis diode array spectrophotometer equipped with a Hellma 1-cm quartz cell. The spectra were recorded in the 200–900 nm wavelength range and the concentration of HA in the supernatant was then evaluated from the absorbance at 500 nm. Calibration curves at the working pH were constructed with several HA solutions having concentrations that ranged between 10 and  $200 \text{ mg L}^{-1}$ . Very good linearity was found in all cases.

The general characterization of the synthesized samples was performed by X-ray diffraction (XRD), FT-IR and the  $\text{N}_2$ -BET method for surface area determination. XRD patterns were obtained using a Bruker D8 X-ray diffractometer with  $\text{CoK}\alpha$  radiation ( $1.7890 \text{ \AA}$ ). Scans were recorded between  $5^\circ$  and  $80^\circ$  ( $2\theta$ ) with a step size of  $0.02^\circ$ . FT-IR spectra were obtained with a Nicolet FT-IR Nexus 470 Spectrophotometer. The samples were dried under vacuum until constant weight was achieved and diluted with KBr powder (1%) before the FT-IR spectra were recorded. The  $\text{N}_2$ -BET adsorption at 77K was measured with a Quantachrome Nova 1200e instrument. Each sample was degassed under vacuum at  $30^\circ\text{C}$  for 60 min prior to analysis. The point of zero charge (PZC) of goethite was measured by potentiometric titrations at three KCl concentrations with a method similar to that reported by Antelo et al. [31].

### 2.2. Adsorption of $PQ^{2+}$ on goethite and HA-goethite

Paraquat adsorption isotherms on goethite were obtained with a batch equilibration procedure using 15 mL polypropylene centrifuge tubes covered with polypropylene caps. Before starting an experiment, a stock goethite suspension ( $23.17 \text{ g L}^{-1}$ ) and a  $PQ^{2+}$  solution ( $5.05 \times 10^{-4} \text{ M}$ ) were prepared by adding the corresponding solid to doubly distilled water. Its pH was then adjusted to the desired value by adding HCl or KOH solutions.  $635 \mu\text{L}$  aliquots of the stock goethite suspension were introduced into the tubes and mixed with varying quantities of  $PQ^{2+}$  and KCl (used as supporting electrolyte) solutions. The range of initial  $PQ^{2+}$  concentration was  $7.78$ – $77.8 \mu\text{M}$ , and the final volume was 7 mL. The suspensions were then mixed on a rotator stirrer (FAES, Argentina) for 4 h and the pH was checked and kept constant by adding small volumes (microliters) of concentrated KOH or HCl solutions. After equilibration, the tubes were centrifuged at 5000 rpm during 20 min and the supernatants were filtered using  $0.2 \mu\text{m}$  pore-diameter cellulose acetate filters (Osmonic) prior to analysis. Adsorbed  $PQ^{2+}$  was calculated from the difference between the initial  $PQ^{2+}$  concentration and the concentration of the herbicide that remained in the supernatant solution.

The procedure to obtain paraquat adsorption isotherms on HA-goethite was equal to the described above, except that the concentration of the stock HA-goethite suspension was  $29.40 \text{ mg L}^{-1}$  and that 0.5 mL of this suspension were introduced into each centrifuge tube. In most experiments the supporting electrolyte was  $1.64 \times 10^{-2} \text{ M}$  KCl (except when effects of ionic strength were investigated). The working temperature was  $25^\circ\text{C}$  (except when effects of temperature were investigated).

Quantification of  $PQ^{2+}$  was performed by UV-vis spectroscopy at 258 nm. Calibration curves at the working pH were also constructed with several  $PQ^{2+}$  solutions having concentration that ranged between 1.55 and  $155 \mu\text{M}$ . Very good linearity was found in all cases.

The adsorption isotherms were fitted using the Langmuir isotherm, which was used in the adsorption of herbicides on several

adsorbent systems [6,32,33]:

$$PQ_{\text{ads}}^{2+} = \frac{q_{\text{max}} K_L PQ_{\text{eq}}^{2+}}{1 + K_L PQ_{\text{eq}}^{2+}}, \quad (1)$$

where  $PQ_{\text{ads}}^{2+}$  is the adsorbed amount of  $PQ^{2+}$  ( $\mu\text{mol g}^{-1}$ ),  $PQ_{\text{eq}}^{2+}$  is the equilibrium concentration of  $PQ^{2+}$  in the supernatant ( $\mu\text{M}$ ),  $q_{\text{max}}$  is the maximum amount of  $PQ^{2+}$  adsorbed ( $\mu\text{mol g}^{-1}$ ), and  $K_L$  is the Langmuir constant ( $\mu\text{M}^{-1}$ ). From the linearized form of the Langmuir equation,

$$\frac{1}{PQ_{\text{ads}}^{2+}} = \frac{1}{q_{\text{max}} K_L PQ_{\text{eq}}^{2+}} + \frac{1}{q_{\text{max}}}, \quad (2)$$

$q_{\text{max}}$ ,  $K_L$  and the correlation coefficient,  $r^2$ , can be calculated.

### 2.3. $PQ^{2+}$ binding to HA by capillary electrophoresis (CE)

$PQ^{2+}$ –HA interaction in solution was followed by CE. Before starting the experiment, stock solutions of HA ( $1000 \text{ mg L}^{-1}$ ) and  $PQ^{2+}$  ( $1.40 \times 10^{-3} \text{ M}$ ) were prepared by adding the corresponding solid to a  $1.30 \times 10^{-3} \text{ M}$  KCl solution at room temperature. The pH of the resulting solutions was then adjusted to pH 8.7 using small volumes of HCl or KOH. In 25 mL balloon flasks, the HA stock solution was diluted to  $500 \text{ mg L}^{-1}$  with KCl solution and was mixed with varying volumes of the  $PQ^{2+}$  solution. The range of  $PQ^{2+}$  concentrations in the experiment was  $0\text{--}700 \mu\text{M}$  and the ionic strength was  $1.30 \times 10^{-3} \text{ M}$ . The mixed solution was shaken for 1–2 min, transferred to 2 mL CE glass vials, injected and analyzed. All sample solutions were filtered using  $0.2 \mu\text{m}$  pore-diameter cellulose acetate filters (Osmonic) prior to injection.

The CE experiments were carried out on a Beckman P/ACE MDQ instrument equipped with a UV–vis diode array detection system. A fused silica capillary tube of 57 cm (effective length 50 cm)  $\times$  75  $\mu\text{m}$  internal diameter was used. The normal polarity mode of the CE system (cathodic pole at the side of detection) was applied. The background electrolyte (BGE) was 44 mM borate buffer (pH 9). Before sample loading, the capillary was conditioned for with 0.1 M NaOH (3 min, 50 psi), doubly distilled  $\text{H}_2\text{O}$  (1 min, 20 psi), and BGE (5 min, 20 psi) at 25 °C. Optimal separation conditions used in this study were separation voltage of 20 kV, 30 °C, hydrodynamic injection (10 s, 5 psi), and the detection wavelength was set at 254 nm. Calibration curves at the working pH were also performed using several  $PQ^{2+}$  solutions (all previously prepared in  $1.30 \times 10^{-3} \text{ M}$  KCl solution) having concentrations that ranged between 140 and 700  $\mu\text{M}$ . Peak area was used for calibration and quantification of bonded  $PQ^{2+}$ .

## 3. Results and discussion

### 3.1. General characteristics of the synthesized goethite and HA–goethite

The specific surface areas of goethite and HA–goethite samples were 57.6 and 38.7  $\text{m}^2 \text{ g}^{-1}$ , respectively. A decrease in the specific surface area with the HA content was also reported by Nachtegaal and Sparks [34] for HA-kaolinite complexes. These authors attributed this decrease to the presence of HA at the kaolinite surface, because HA has a surface area that is much lower than that of the mineral. This might be also the case for the HA–goethite sample. The presence of adsorbed HA may also block some pores of the solid and induce particle aggregation, processes that could also contribute to the decrease in the area. Fig. 1 shows the X-ray diffractogram of the goethite sample. It also shows the position of goethite peaks as calculated from data published by Hazemann et al. [35]. The peak coincidence and the absence of extra peaks

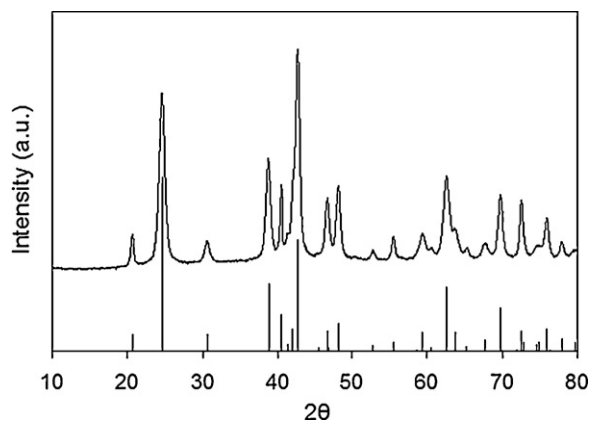


Fig. 1. XRD patterns of the synthesized goethite. Vertical lines show the results reported by Hazemann et al. [35] for a well-crystallized goethite.

in the experimental diffractogram indicate that the studied sample was a well-crystallized goethite, and that no other crystalline phases were detected by XRD. Goethite characteristic peaks are located at 24.66°, 38.78°, 42.80° and 62.60° and are associated to the planes (1 1 0), (1 3 0), (1 1 1) and (2 2 1), respectively [35]. The point of zero charge of the goethite was 8.9, indicating that the net surface charge is positive at pH <8.9 and negative at pH >8.9 [31]. Transmission FT-IR spectra of HA, goethite and HA–goethite are shown in Fig. 2. The most important features of HA are a broad band at  $3400 \text{ cm}^{-1}$  associated to OH stretching of OH groups, a peak at  $2933 \text{ cm}^{-1}$  due to aliphatic C–H stretching, a shoulder at  $1716 \text{ cm}^{-1}$  attributed to C=O stretching of COOH and ketones, a strong peak at  $1615 \text{ cm}^{-1}$  associated to structural vibrations of aromatic C=C and antisymmetrical stretching of  $\text{COO}^-$  groups, a medium intensity peak at  $1400 \text{ cm}^{-1}$  due to symmetrical stretching of  $\text{COO}^-$  groups and another one at  $1230 \text{ cm}^{-1}$  attributed to C–O stretching and OH bending of COOH groups [36]. Goethite shows characteristic absorption bands at around 3419 and  $3145 \text{ cm}^{-1}$  due to OH stretching, 890 and  $795 \text{ cm}^{-1}$  due to OH bending and  $638 \text{ cm}^{-1}$  due to Fe–O stretching [11,37,38]. Some differences can be observed in the FT-IR spectra of HA–goethite. One such difference is the decrease in the intensity of the  $3419 \text{ cm}^{-1}$  band, corresponding to the O–H stretching of the hydroxyl surface groups. In addition, the band situated at  $1632 \text{ cm}^{-1}$  corresponding to water molecules at the mineral surface is shifted towards lower wavelength with decrease in intensity. Similar results were obtained by Gu et al. [39,40] for the adsorption and desorption of organic matter on iron oxides. According to these authors, these changes are significant evidence that HA interacts with the goethite surface through hydrogen bonds and surface

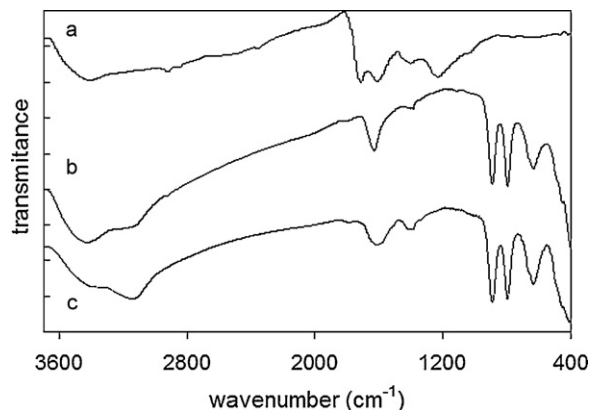
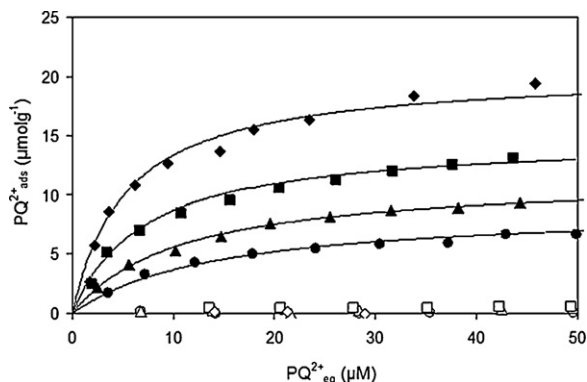


Fig. 2. Infrared spectra of (a) HA, (b) goethite, and (c) HA–goethite.



**Fig. 3.** Effect of pH on the adsorption of  $PQ^{2+}$  on goethite (open symbols) and HA-goethite (solid symbols). Circles, pH 4.5; triangles, pH 6; squares, pH 7.5; and diamonds, pH 8.7. Lines show predictions of Eq. (1) with parameters from Table 1.

complexation reactions, mainly between carboxylate and phenolate groups present in the HA molecules and active sites of goethite (surface Fe and OH).

### 3.2. Adsorption of $PQ^{2+}$ on goethite and HA-goethite

Fig. 3 shows the effects of pH on the adsorption of  $PQ^{2+}$  on goethite and HA-goethite at 25 °C and  $1.64 \times 10^{-2}$  M ionic strength. The adsorption on goethite was negligible in all experimental conditions (pH range between 4.5 and 8.7). At pH values lower than the PZC, the goethite surface has a net positive charge and electrostatics restricts the adsorption of the dication. In addition,  $PQ^{2+}$  does not have the ability of transition metal cations to form inner-sphere surface complexes with surface sites of goethite and overcome electrostatics, as seen by Saito et al. [41] for the adsorption of  $Cu^{2+}$  on goethite. The experimental results are in agreement with those reported by Hseu et al. [42], who showed that Fe oxides reduced the adsorption of  $PQ^{2+}$  on different clayey soils of Taiwan by blocking the adsorption sites.

On the contrary to the adsorption on goethite,  $PQ^{2+}$  adsorption readily takes place on HA-goethite, showing that the presence of HA favorably affects this process. The shape of the isotherms is similar to the shape of the isotherms reported by Rytwo et al. [43], Iglesias et al. [9] and Burns et al. [44] for the adsorption of  $PQ^{2+}$  on negatively charged clays, HA and Ca-humate, respectively. Fig. 3 also shows that the adsorption on HA-goethite is strongly dependent on the pH. It is relatively high at high pH and decreases significantly at lower pH values. No desorption of HA could be detected in all these experiments.

$PQ^{2+}$  adsorption on HA-goethite could take place either by direct binding to the uncovered goethite surface or by direct binding to HA molecules. The first case does not appear to be important under our experimental conditions since it was shown that attachment to the bare goethite surface does not take place. The second case seems to be the most probable. The direct binding between  $PQ^{2+}$  and adsorbed HA molecules generates ternary surface species goethite-HA- $PQ^{2+}$ , whose formation is mainly driven by  $PQ^{2+}$ -HA interactions. The herbicide contains a delocalized  $\pi$ -electron system and thus some  $\pi$ -bonding could be postulated between  $PQ^{2+}$  and regions with aromatic rings in the adsorbed HA molecules. In addition, electrostatic interactions are also possible between HA and  $PQ^{2+}$ , where negatively charged groups (carboxylates and phenolates) of adsorbed HA could bind the dication by forming ionic pairs or outer-sphere complexes. The increase in adsorption by increasing pH is qualitatively understood irrespective of whether the binding process is  $\pi$ -bonding or ionic pairs or outer-sphere complexes formation. If it is  $\pi$ -bonding, increasing the pH will increase the degree of dissociation of HA, leading to an increased

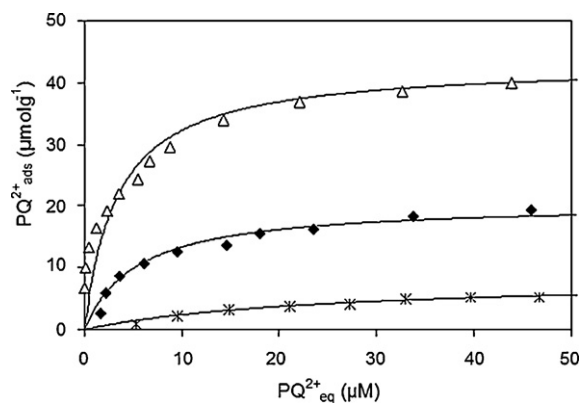


**Fig. 4.** Effect of ionic strength on the adsorption of  $PQ^{2+}$  on HA-goethite at pH 8.7. KCl concentrations: open triangles,  $1.30 \times 10^{-3}$  M; solid diamonds,  $1.64 \times 10^{-2}$  M; and stars, 0.1 M. Lines show predictions of Eq. (1) with parameters from Table 1.

electrostatic attraction between  $PQ^{2+}$  and HA-goethite and a higher adsorption. If the binding mechanism is formation of ionic pairs or outer-sphere complexes between negatively charged groups and  $PQ^{2+}$ , the increased amount of carboxylates and phenolates at high pH will enhance the adsorption.

The effects of ionic strength on the adsorption of  $PQ^{2+}$  on HA-goethite at pH 8.7 and 25 °C are shown in Fig. 4. The adsorption depends on the ionic strength, decreasing as the ionic strength increases. These results suggest that formation of ionic pairs or outer-sphere complexes is the prevailing adsorption process: the competition between  $PQ^{2+}$  and  $K^{+}$  for negatively charge groups leads to an important decrease in  $PQ^{2+}$  adsorption by increasing  $K^{+}$  concentration. The results resemble those reported by Tsai et al. [7] for the adsorption of  $PQ^{2+}$  on activated clays, where competition between  $PQ^{2+}$  and electrolyte cations was proposed to play a key role. Adsorption by  $\pi$ -bonding should not be strongly affected by changing the supporting electrolyte concentration, and thus this is not the prevailing adsorption process.

The effects of temperature on the adsorption of  $PQ^{2+}$  on HA-goethite at pH 8.7 are shown in Fig. 5.  $PQ^{2+}$  adsorption is not significantly affected by varying the temperature from 5 to 45 °C, and the maximum uptake was between 19.5 and 20.5  $\mu\text{mol g}^{-1}$  at all investigated temperatures. Several reports exist about the effect of temperature in the adsorption behavior of  $PQ^{2+}$  on different adsorbents. Tsai et al. [7] showed that the adsorption of  $PQ^{2+}$  on clay minerals increased by increasing temperature suggesting that a chemisorption-like process may play an important role in the  $PQ^{2+}$ -clay adsorbent system. These observations are signifi-

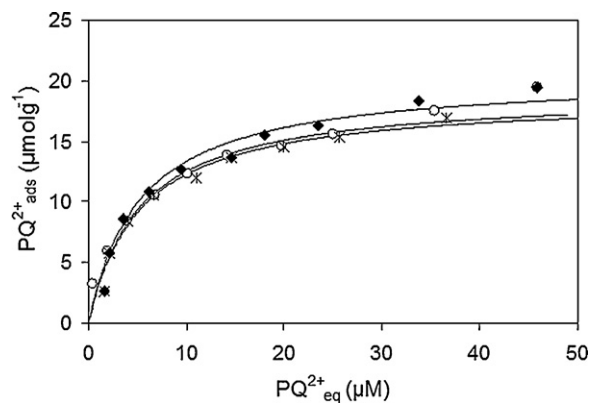


**Fig. 5.** Effect of temperature on the adsorption of  $PQ^{2+}$  on HA-goethite at pH 8.7. Open circles, 45 °C; solid diamonds, 25 °C; and stars, 5 °C. Lines show predictions of Eq. (1) with parameters from Table 1.

**Table 1**  
Best-fit parameters for Eq. (1).

$T$ (°C)	pH	$I$ (M)	$q_{\max}$ ( $\mu\text{mol g}^{-1}$ )	$K_L$ ( $\mu\text{M}^{-1}$ )	$r^2$
25	4.5	0.0164	8.90	0.070	0.989
25	6.0	0.0164	11.49	0.094	0.998
25	7.5	0.0164	14.87	0.140	0.997
25	8.7	0.0164	20.44	0.187	0.990
25	8.7	0.0013	43.14	0.226	0.992
25	8.7	0.1000	8.33	0.040	0.994
5	8.7	0.0164	18.70	0.190	0.990
45	8.7	0.0164	19.04	0.192	0.984

cantly different from those reported by Nakamura et al. [8], who reported that  $\text{PQ}^{2+}$  adsorption on activated carbon decreased by increasing temperature (physical adsorption). None of these mechanisms are in agreement with data shown in Fig. 5, indicating that temperature effects on  $\text{PQ}^{2+}$  adsorption are strongly dependent on the type of adsorbent. The independence of the adsorption of  $\text{PQ}^{2+}$  with the temperature is not inconsistent with formation of ionic pairs or outer-sphere complexes, where there is competition with the cations of the supporting electrolyte. If changes in temperature affect in a similar way the affinity of  $\text{PQ}^{2+}$  and  $\text{K}^+$  for negatively charged sites, there will be no significant temperature effects by changing the temperature.

In Figs. 3–5, symbols correspond to data points whereas solid lines correspond to the best-fitting Langmuir isotherms calculated by adjusting the parameters  $q_{\max}$  and  $K_L$ . These parameters are listed in Table 1. Even though the formulated model is rather simple, it can fit reasonably well the adsorption of  $\text{PQ}^{2+}$ , i.e., the goodness-of-fit of Eq. (1) was checked through the  $r^2$  values, which was between 0.984 and 0.997 in all cases. Changes in pH and ionic strength result in important changes in the adsorption isotherm, i.e.,  $q_{\max}$  and  $K_L$  increase as pH increases or ionic strength decreases. On the other hand, significant changes in these parameters were not obtained by changing the temperature from 5 to 45 °C.

### 3.3. $\text{PQ}^{2+}$ binding to HA by capillary electrophoresis (CE)

The overall results suggest that HA molecules are the responsible for the adsorption of  $\text{PQ}^{2+}$  on HA–goethite and that the  $\text{PQ}^{2+}$  molecules are directly attached to the adsorbed HA. Therefore, CE was used to determine if really exists an interaction between  $\text{PQ}^{2+}$  and HA in absence of goethite. CE is an effective tool in the analysis and characterization of herbicides and their metabolites of degradation, humic substances, and interaction between them [26,45,46]. Fig. 6 shows the electropherograms corresponding to  $\text{PQ}^{2+}$ , HA, and the mixture of HA and  $\text{PQ}^{2+}$ . The electropherograms

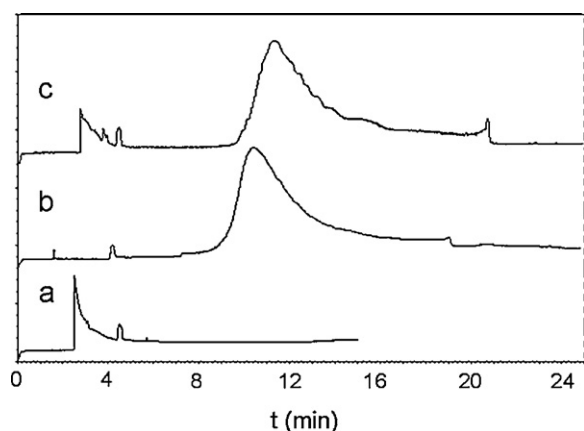


**Fig. 6.** Electropherograms corresponding to: (a)  $\text{PQ}^{2+}$ ,  $1.40 \times 10^{-3}$  M; (b) HA,  $500 \text{ mg L}^{-1}$ ; and (c)  $\text{PQ}^{2+}$ –HA mixture solutions.

can be evaluated by plotting the absorbance as a function of migration time.

$\text{PQ}^{2+}$  appears as a broad peak at migration time of 3 min, electroosmotic flow (EOF) at 4.5 min, and HA at 10.4 min. The broad not-resolved peak of HA is due to the fact that HA is constituted by a complex and heterogeneous mixture of molecules. Addition of the herbicide to the humic solution (electropherogram c) results in a decrease in the intensity of the  $\text{PQ}^{2+}$  peak and in a shift of the HA peak towards higher migration times. The decrease in peak intensity of  $\text{PQ}^{2+}$  is clear evidence that the herbicide concentration in solution decreases by direct interaction with the humic molecules. Similar results were obtained by Pacheco et al. [46] for addition of  $\text{PQ}^{2+}$  to a  $100 \text{ mg L}^{-1}$  HA solution. According to these authors,  $\text{PQ}^{2+}$  binds to HA molecules by ionic bonds resulting in charge neutralization.

From electropherograms as the illustrated in Fig. 6, it is possible to quantify the binding of  $\text{PQ}^{2+}$  to HA at different initial concentrations of  $\text{PQ}^{2+}$  by integrating the  $\text{PQ}^{2+}$  absorption peak. These results are shown in Fig. 7. Fig. 7a compares the binding of the herbicide to HA in solution with the adsorption on HA–goethite under similar conditions. The binding to HA is higher than the

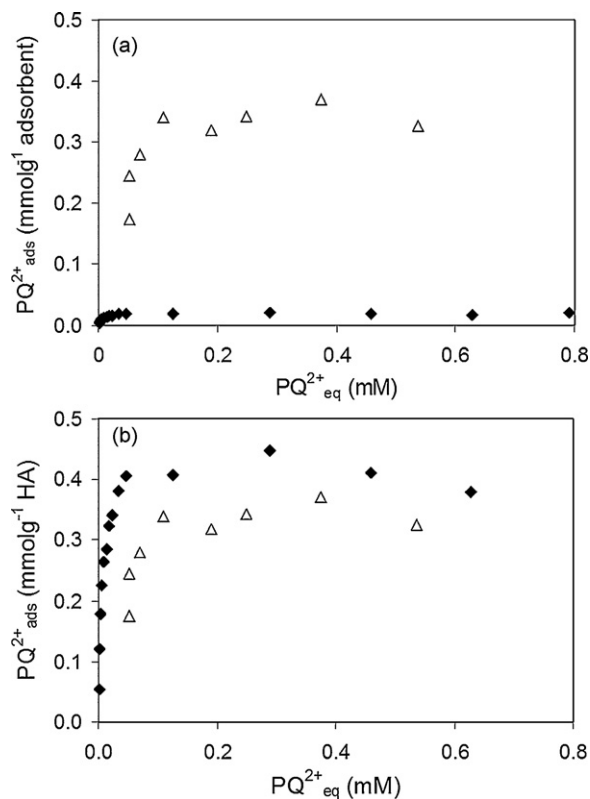


**Fig. 7.** Adsorption isotherms of  $\text{PQ}^{2+}$  on HA (open triangles) and HA–goethite (solid diamonds) at pH 8.7 expressed in: (a) amount of bonded  $\text{PQ}^{2+}$  per mass of adsorbent; and (b) amount of bonded  $\text{PQ}^{2+}$  per mass of HA.

adsorption on HA–goethite. However, if the data are expressed as bonded/adsorbed  $PQ^{2+}$  per mass of HA, without considering the mass of goethite, the curves result to be rather similar (Fig. 7b). This rather good agreement between the curves confirms the fact that  $PQ^{2+}$  adsorption on HA–goethite takes place mainly on adsorbed HA molecules, and that goethite is mainly acting as a support for HA. Actually, Fig. 7b shows that adsorbed HA molecules have a slightly lower binding capacity than HA molecules in solution. This can be easily understood since some reactive groups (carboxylate and phenolate) of adsorbed HA should be blocked because they may be involved in the interaction with the goethite surface.

#### 4. Conclusions

The results shown in this article reveal that the adsorption of  $PQ^{2+}$  on the bare goethite surface is negligible. The electrostatic repulsion between  $PQ^{2+}$  and positively charged goethite surface seems to be the main factor that prevents the attachment of this herbicide. However, the presence of HA adsorbed to the goethite surface strongly enhance the adsorption capability of  $PQ^{2+}$ .

The adsorption of  $PQ^{2+}$  on HA–goethite takes place by direct binding of the herbicide to adsorbed HA molecules and thus ternary surface species of the type goethite–HA– $PQ^{2+}$  are formed. The adsorption process is mainly formation of ionic pairs or outer-sphere complexes between negatively charged groups of HA and  $PQ^{2+}$ , as deduced from adsorption experiments performed at different ionic strengths.

Capillary electrophoresis demonstrates that direct binding between  $PQ^{2+}$  and HA occurs, and allowed to construct binding isotherms of  $PQ^{2+}$  to HA molecules solution.

The obtained results have a significant importance in environmental processes, where goethite plays a key role. Goethite is known to be a very good adsorbent for anionic species (phosphate, arsenate, carbonate, humic substances, etc.). However, since goethite in nature also contains adsorbed HA molecules, the goethite–HA system may also act as a good adsorbent for cationic herbicides. This will not only benefit the deactivation of the herbicides but also reduce their leaching and transport through groundwater.

#### Acknowledgments

This work was financed by SECyT-UNS, CONICET and ANPCYT. The authors thank Olga Pieroni for the IR spectra. M. Brigante thanks CONICET for the doctoral fellowship.

#### References

- [1] R.H. Bromilow, Paraquat and sustainable agriculture, *Pest Manag. Sci.* 60 (2004) 340–349.
- [2] C.M. Chen, A.C. Lua, Lung toxicity of paraquat in the rat, *J. Toxicol. Environ. Health A* 59 (2000) 477–487.
- [3] R.J. Dinis-Oliveira, F. Remião, H. Carmo, J.A. Duarte, A. Sanchez Navarro, M.L. Bastos, F. Carvalho, Paraquat exposure as an etiological factor of Parkinson's disease, *Neurotoxicology* 27 (2006) 1110–1122.
- [4] J.M. Kleijn, E. Rouwendal, H.P. van Leeuwen, J. Lyklema, A kinetic model for the  $Ru(bipy)_3^{2+}/MV^{2+}/EDTA$ /colloidal  $RuO_2$  system for photogeneration of hydrogen, *J. Photochem. Photobiol. A* 44 (1988) 29–50.
- [5] M.N. Jones, N.D. Bryan, Colloidal properties of humic substances, *Adv. Colloid Interface Sci.* 78 (1980) 1–48.
- [6] Y. Seki, K. Yurdaoç, Paraquat adsorption onto clays and organoclays from aqueous solution, *J. Colloid Interface Sci.* 287 (2005) 1–5.
- [7] W.T. Tsai, C.W. Lai, Adsorption of herbicide paraquat by clay mineral regenerated from spent bleaching earth, *J. Hazard. Mater. B* 134 (2006) 144–148.
- [8] T. Nakamura, N. Kawasaki, H. Ogawa, S. Tanada, M. Kogirima, M. Imaki, Adsorption removal of paraquat and diquat onto activated carbon at different adsorption temperature, *Toxicol. Environ. Chem.* 70 (1999) 275–280.
- [9] A. Iglesias, R. López, D. Gondar, J. Antelo, S. Fiol, F. Arce, Effect of pH and ionic strength on the binding of paraquat and MCPA by soil fulvic and humic acids, *Chemosphere* 76 (2009) 107–113.
- [10] L. Clausen, I. Fabricius, Atrazine, isoproturon, mecoprop, 2,4-D, and bentazone adsorption onto iron oxides, *J. Environ. Qual.* 30 (2001) 858–869.
- [11] R.M. Cornell, U. Schwertmann, *The Iron Oxides. Properties, Reactions, Occurrence, and Uses*, VCH, Weinheim, Germany, 1996.
- [12] M. Villalobos, A. Pérez-Gallego, Goethite surface reactivity: a macroscopy investigation unifying proton, chromate, carbonate, and lead (II), *J. Colloid Interface Sci.* 326 (2008) 307–323.
- [13] T.E. Alcacio, D. Hesterberg, J.W. Chou, J.D. Martin, S. Beauchemin, D.E. Sayers, Molecular scale characteristics of Cu(II) bonding in goethite–humate complexes, *Geochim. Cosmochim. Acta* 65 (2001) 1355–1366.
- [14] G. Abate, J.C. Penteado, J.D. Cuzzi, G.C. Vitti, J. Lichtig, J.C. Masini, Influence of humic acid on adsorption and desorption of atrazine, hydroxyatrazine, deethylatrazine, and deisopropylatrazine onto a clay-rich soil sample, *J. Agric. Food Chem.* 52 (2004) 6747–6754.
- [15] G. Zanini, C. Maneiro, C. Waiman, J.A. Galantini, R.A. Rosell, Adsorption of metsulfuron-methyl on soils under no-till system in semiarid Pampean Region, Argentina, *Geoderma* 149 (2009) 110–115.
- [16] M. Bekbolet, O. Yenigun, I. Yucel, Sorption studies of 2,4-D on selected soils, *Water Air Soil Pollut.* 111 (1999) 75–88.
- [17] R. Sutton, G. Sposito, Molecular structure in soil humic substances: the new view, *Environ. Sci. Technol.* 39 (2005) 9009–9015.
- [18] A. Piccolo, The supramolecular structure of humic substances, *Soil Sci.* 166 (2001) 810–832.
- [19] N. Senesi, V. D'Orazio, T. Miano, Adsorption mechanisms of s-triazine and bipyridylum herbicides on humic acids from hop field soils, *Geoderma* 66 (1995) 273–283.
- [20] M. Brigante, G. Zanini, M. Avena, Effect of pH, anions and cations on the dissolution kinetics of humic acid particles, *Colloid Surf. A* 347 (2009) 180–186.
- [21] Y.Y. Chien, E.G. Eun-Gyeong Kim, W.F. Bleam, Paramagnetic relaxation of atrazine solubilized by rumic micellar solutions, *Environ. Sci. Technol.* 31 (1997) 3204–3208.
- [22] U. Klaus, T. Pfeifer, M. Spiteller, APCI-MS/MS: a powerful tool for the analysis of bound residues resulting from the interaction of pesticides with DOM and humic substances, *Environ. Sci. Technol.* 34 (2000) 3514–3520.
- [23] M.J. Piana, K.O. Zahir, Investigation of metal ions binding of humic substances using fluorescence emission and synchronous-scan spectroscopy, *J. Environ. Sci. Health B* 35 (2000) 87–102.
- [24] L. Martin-Neto, D. Gomes Tragheta, C.M.P. Vaz, S. Crestana, G. Sposito, On the interaction mechanisms of atrazine and hydroxyatrazine with humic substances, *J. Environ. Qual.* 30 (2001) 520–525.
- [25] N. Hesketh, M.N. Jones, E. Tipping, The interaction of some pesticides and herbicides with humic substances, *Anal. Chim. Acta* 327 (1996) 191–201.
- [26] Ph. Schmitt-Kopplin, J. Junkes, Capillary zone electrophoresis of natural organic matter, *J. Chromatogr. A* 998 (2003) 1–20.
- [27] D. Gajdošová, K. Novotná, P. Prošek, J. Havel, Separation and characterization of humic acids from Antarctica by capillary electrophoresis and matrix-assisted laser desorption ionization time-of-flight mass spectroscopy. Inclusion complexes of humic acids with cyclodextrins, *J. Chromatogr. A* 1014 (2003) 117–127.
- [28] M.übner, V. Lepane, M. Lopp, M. Kaljurand, Electrophoretic aggregation of humic acid, *J. Chromatogr. A* 1045 (2004) 253–258.
- [29] R.J. Atkinson, A.M. Posner, J.P. Quirk, Adsorption of potential-determining ions at the ferric oxide–aqueous electrolyte interface, *J. Phys. Chem.* 71 (1967) 550–558.
- [30] N.H. Solá, S.B. Ceppi, R. Sereno, Characterization and comparative studies of humic acids of soil with different cultivate practises, *Ciencia del Suelo* 6 (1988) 108–112 (published in Spanish).
- [31] J. Antelo, M. Avena, S. Fiol, R. López, F. Arce, Effects of pH and ionic strength on the adsorption of phosphate and arsenate at the goethite–water interface, *J. Colloid Interface Sci.* 285 (2005) 476–486.
- [32] B. Barja, M. Dos Santos Afonso, Aminomethylphosphonic acid and glyphosate adsorption on goethite: a comparative study, *Environ. Sci. Technol.* 39 (2005) 585–592.
- [33] P. Chingombe, B. Saha, R.J. Wakeman, Sorption of atrazine on conventional and surface modified activated carbons, *J. Colloid Interface Sci.* 302 (2006) 408–416.
- [34] M. Nachtegaal, D.L. Sparks, Nickel sequestration in a kaolinite–humic acid complex, *Environ. Sci. Technol.* 37 (2003) 529–534.
- [35] J.L. Hazemann, J.F. Berar, A. Manceau, Rietveld studies of the aluminium–iron substitution in synthetic goethite, *Mater. Sci. Forum* 79 (1991) 821–826.
- [36] F.J. Stevenson, *Humus Chemistry: Genesis, Composition, Reactions*, Wiley, New York, 1994.
- [37] M. Villalobos, J.O. Leckie, Surface complexation modeling and FTIR study of carbonate adsorption to goethite, *J. Colloid Interface Sci.* 235 (2001) 15–32.
- [38] S. Krehula, S. Musić, Influence of cobalt ions on the precipitation of goethite in highly alkaline media, *Clay Miner.* 43 (2008) 95–105.
- [39] B. Gu, J. Schmitt, Z. Chen, L. Liang, J.F. McCarthy, Adsorption and desorption of natural organic matter on iron oxide: mechanisms and models, *Environ. Sci. Technol.* 28 (1994) 38–46.
- [40] B. Gu, J. Schmitt, Z. Chen, L. Liang, J.F. McCarthy, Adsorption and desorption of different organic matter fractions on iron oxide, *Geochim. Cosmochim. Acta* 59 (1995) 219–229.
- [41] T. Saito, L. Koopal, W.H. van Riemsdijk, S. Nagasaki, S. Tanaka, Adsorption of humic acid on goethite: isotherms, charge adjustments, and potential profiles, *Langmuir* 20 (2004) 689–700.

- [42] Z.Y. Hseu, S.H. Jien, S.F. Cheng, Sorption of paraquat on clay components in Taiwan's oxisol, *J. Environ. Sci. Health B* 38 (2003) 441–449.
- [43] G. Rytwo, S. Nir, L. Margulies, Adsorption and interactions of diquat and paraquat with montmorillonite, *Soil Sci. Soc. Am. J.* 60 (1996) 601–610.
- [44] I.G. Burns, M.B.H. Hayes, M. Stacey, Studies of the adsorption of paraquat on soluble humic fractions by gel filtration and ultrafiltration techniques, *Pest. Sci.* 4 (1973) 629–641.
- [45] M. Corbera, M. Hidalgo, V. Salvadó, P.P. Wiczorek, Determination of glyphosate and aminomethylphosphonic acid in natural water using the capillary electrophoresis combined with enrichment step, *Anal. Chim. Acta* 540 (2005) 3–7.
- [46] M.L. Pacheco, E.M. Peña-Méndez, J. Havel, Supramolecular interactions of humic acids with organic and inorganic xenobiotics studied by capillary electrophoresis, *Chemosphere* 51 (2003) 95–108.